Use of Single-Turnover Kinetics To Study Bulky Adduct Bypass by T7 DNA Polymerase†

Janet E. Lindsley*,‡ and Robert P. P. Fuchs

Groupe de Cancérogenèse et de Mutagenèse Moléculaire et Structurale, Institut de Biologie Moléculaire et Cellulaire du CNRS, 15, rue René Descartes, 67084 Strasbourg, France

Received August 9, 1993; Revised Manuscript Received November 2, 1993®

ABSTRACT: The mechanism by which T7 DNA polymerase (exo⁻) bypasses *N*-2-acetylaminofluorene (AAF) and *N*-2-aminofluorene (AF) adducts was studied by single-turnover kinetics. These adducts are known to be mutagenic in several cell types, and their bypass was studied in the framework of understanding how they promote mutations. Synthetic primer/templates were made from a template sequence containing a single guanine, to which the adducts were covalently attached, and one of three primers whose 3′ ends were various distances from the adduct in the annealed substrates. Upon approaching the site of either adduct, the polymerase was found to add nucleotides as rapidly as to unmodified primer/templates, until just opposite the lesion. The incorporation rate of dCTP (at 100 μM) opposite AF-dG or AAF-dG was approximately 5×10^4- and 4×10^6-fold slower, respectively, than incorporation at the same position into an unmodified primer/template. The polymerase dissociated from the sites of the adducts at approximately the same rate that it dissociated from unmodified DNA. Correct nucleotide incorporation was favored both opposite and immediately after AF-dG. However, at both positions, dATP was the most rapidly misincorporated nucleotide. Misincorporation of dATP was more rapid than correct nucleotide incorporation both opposite and immediately after AAF-dG. These results are discussed in terms of the effects of AF and AAF adducts *in vivo*.

In vivo, DNA is reactive toward a variety of agents, resulting in genomes that contain lesions and covalent adducts. Repair of these modifications is often not complete prior to DNA replication, and, depending their nature, they may increase the frequency by which a passing polymerase makes mutations. The chemical carcinogen *N*-2-acetylaminofluorene (AAF) forms two major bulky DNA adducts *in vivo*, *N*-(deoxyguanosin-8-yl)-2-acetylaminofluorene (AAF-dG) and its deacetylated derivative, AF-dG, both of which increase the frequency of mutations [see Figure 1 for structures of AAF-dG and AF-dG; see Daune et al. (1981) and Kriek (1992) for reviews]. Although the two adducts differ only in an acetyl group, their effects on DNA structure are proposed to be quite different. When attached to guanines within random sequences, AAF is thought to induce local denaturation, with the fluorene ring inserted between the base pairs and the guanine rotated outside of the double helix (Fuchs & Daune, 1972; Fuchs et al., 1976; Grunberger & Weinstein, 1979; O'Handley et al., 1993). By contrast, DNA containing an AF-dG is not greatly distorted (Daune et al., 1981). In bacteria, AAF and AF have been shown to induce primarily frame-shift and substitution mutations, respectively (Fuchs et al., 1981; Koffel-Schwartz et al., 1984; Bichara & Fuchs, 1985). Both frame-shift mutations and base substitutions are induced by these adducts in eukaryotic cells (Mah et al., 1989, 1991). In all cases, the most frequently found substitution mutations were G·C → T·A transversions.

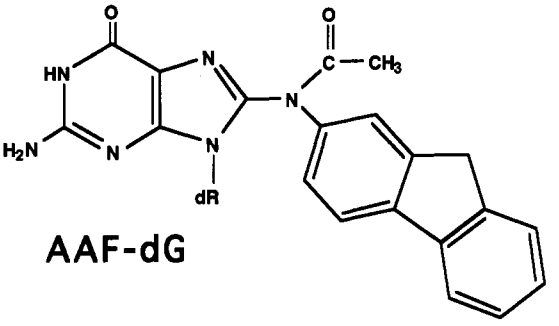

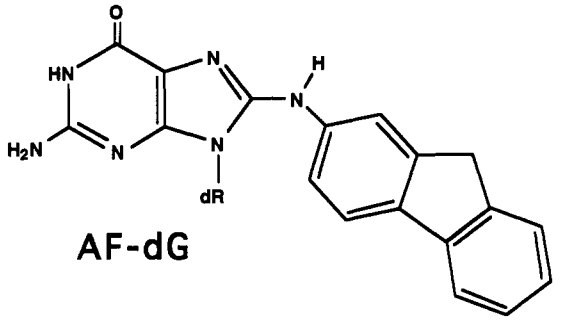

FIGURE 1: Chemical structures of *N*-(deoxyguanosin-8-yl)-*N*-(2-acetylamino)fluorene, AAF-dG, and *N*-(deoxyguanosin-8-yl)-*N*-(2-amino)fluorene, AF-dG. dR represents the deoxyribose ring.

Several groups have studied the effects of AF and AAF lesions *in vitro* using purified DNA polymerases and modified primer/templates and have found indeed that the adducts change the efficiency and/or rate of polymerization (O'Conner & Stohrer, 1985; Michaels et al., 1987, 1991; Strauss & Wang, 1990; Belguise-Valladier & Fuchs, 1994). However, without

† Supported in part by grants from the Association pour la Recherche sur le Cancer (Grant No. 6143) and the Human Frontier Science Program and by American Cancer Society Postdoctoral Fellowship No. PF-3534 (J.E.L.).

* Author to whom correspondence should be addressed.

‡ Present address: Department of Biochemistry, University of Utah, Salt Lake City, UT 84132.

® Abstract published in *Advance ACS Abstracts*, December 15, 1993.

[1] Abbreviations: AAF, *N*-2-acetylaminofluorene; AAF-dG, *N*-(deoxyguanosin-8-yl)-2-acetylaminofluorene; AF, *N*-2-aminofluorene; AF-dG, *N*-(deoxyguanosin-8-yl)-2-aminofluorene; BSA, bovine serum albumin; dNTP, deoxynucleoside 5′-triphosphate; DTT, dithiothreitol; Tris, tris(hydroxymethyl)aminomethane.

0006-2960/94/0433-764$04.50/0

a detailed understanding of how the polymerase incorporates and misincorporates nucleotides into normal DNA, the underlying mechanism of the altered polymerase activity in bypassing a lesion remains obscure. The T7 DNA polymerase was chosen for the present studies because it is a fast, accurate, processive polymerase and the minimal kinetic pathway by which it incorporates both correct and incorrect nucleotides has been well studied, primarily by Johnson and co-workers (Donlin et al., 1991; Patel et al., 1991; Wong et al., 1991; Johnson, 1992). These studies have led to the suggestion that the fidelity of the polymerization step in the nucleotide discrimination is caused by an "induced fit" of the enzyme in the ternary complex if, and only if, the correct nucleotide is present (Wong et al., 1991; Johnson, 1992). With this model available for the mechanism of normal nucleotide incorporation and misincorporation, the steps altered by the presence of an adduct in the template can begin to be evaluated.

In this paper, we present a series of kinetic experiments using purified exo$^-$ T7 DNA polymerase and synthetic oligonucleotide primer/templates, with and without AF or AAF adducts, designed to elucidate the effects of the adducts on DNA polymerization. The exo$^-$ derivative of the polymerase created in the Johnson lab was found to have polymerization properties identical to those of the wild-type enzyme while lacking the highly active nuclease (Patel et al., 1991). As is true for all processive polymerases, the rate of incorporation of a small number of nucleotides (<1000) by T7 DNA polymerase, as measured by multiple turnover, steady-state kinetics, is dominated by the rate-limiting step of enzyme–DNA dissociation. Single-turnover kinetics were used in this study to avoid the problem of measuring only the rate of the step limiting in enzyme turnover. This is especially important when comparing reactions with different overall rate-limiting steps, as is found to be the case for polymerization on unmodified versus AF- or AAF-modified primer/templates. Since the T7 DNA polymerase has been shown to normally incorporate a nucleotide once every ~4–5 ms (Patel et al., 1991), rapid quench-flow was used to measure the incorporation rate on control, unmodified primer/templates and to follow the rate of approach to the adduct on modified primer/templates. The rates of nucleotide incorporation opposite and immediately after either adduct were found to be several orders of magnitude slower than the normal rate, allowing time points to be taken manually. These techniques were used to follow (1) the rates of multiple nucleotide incorporation in the vicinity of the adducts and (2) the incorporation rates of single correct and incorrect nucleotides opposite and immediately following the adducts.

EXPERIMENTAL PROCEDURES

Materials. The DNA oligonucleotides used for primer/templates were synthesized on an Applied Biosystems 380B DNA synthesizer (see Table 1 for sequences). All four dNTPs (>99.4% pure) were purchased from Pharmacia; the [α-^{32}P]-dNTPs and the [γ-^{32}P]ATP were from Amersham. The BSA (fraction V) was from Sigma.

Preparation of Templates Modified with AAF and AF. Each of the synthetic DNA oligonucleotides was first purified by polyacrylamide gel electrophoresis. Approximately 0.5 mg of the 44-mer template was treated with *N*-acetoxy-*N*-2-acetylaminofluorene (0.1 mg) as previously described (Koehl et al., 1989), except that the time of incubation was extended to 1 h. The oligonucleotide containing a single AAF adduct was purified by reverse-phase HPLC on a Nucleosil C18 column using a linear gradient of 22.5–45% methanol in triethylamine acetate (0.05 M, pH 6). The position of the adduct and the reaction yield were tested by treating the templates with T4 DNA polymerase; the 3′ → 5′ exonuclease activity of this enzyme degrades the template up to the position of the adduct (Fuchs, 1984). A portion of the 44-AAF-mer (0.2 mg) was deacetylated to 44-AF-mer by incubation with NaOH (1 N) and β-mercaptoethanol (0.25 M) at 37 °C until the increase in absorbance at 325 nm reached a plateau (40 min) (Shibutani et al., 1991). The reaction was then neutralized by adding one-tenth volume of a 2 M sodium acetate/10 M acetic acid solution and precipitating with three volumes of ethanol. The product, 44-AF-mer, was stored in TE plus 10 mM DTT.

Table 1: Synthetic Primer/Template Substrates[a]

25/44 mer	5′ GATTGGTATGATGGTGATTGGTTGA CTAACCATACTACCACTAACCAACTACCACGACAACTTACTACC 5′
30/44 mer	5′ GATTGGTATGATGGTGATTGGTTGATGGTG CTAACCATACTACCACTAACCAACTACCACGACAACTTACTACC 5′
31/44 mer	5′ GATTGGTATGATGGTGATTGGTTGATGGTGC CTAACCATACTACCACTAACCAACTACCACGACAACTTACTACC 5′

[a] The enlarged "G" represents the solitary guanine in the template strand; this is the position of the covalently attached AF and AAF adducts in modified primer/templates.

Preparation of Primer/Templates. Prior to primer/template annealing, 5′ ends of the unmodified and modified templates were phosphorylated with nonradiolabeled ATP and T4 polynucleotide kinase (New England Biolabs) to block future radiolabeling (see below). Approximately equal molar quantities (as determined by absorbance at 260 nm) of primer and template strands were annealed and purified from 20% nondenaturing polyacrylamide gels.

The concentration of all 25/44-mer and unmodified 30- and 31/44-mer primer/templates was determined by incorporation of the single next correct [α-^{32}P]dNTP exactly as described (Patel et al., 1991). After the concentration was known, the 5′ end of the primer was labeled with [γ-^{32}P]ATP (3000 Ci/mmol) and polynucleotide kinase; since the 5′ end of the template was previously phosphorylated, the majority of the label was directed to the 5′ end of the primer.

Due to the inefficiency of nucleotide incorporation into the modified 30- and 31/44-mer primer/templates, the concentration of these substrates was determined by a separate procedure. The concentrations of the 30- and 31-mer primers were determined prior to template annealing by absorbance. The 5′ ends of these primers were phosphorylated with [γ-^{32}P]-ATP (3000 Ci/mmol) and T4 polynucleotide kinase. The efficiency of the kinase reaction was determined by DE81 filter binding as described (Patel et al., 1991). The primer/templates were annealed and gel purified as described above, and their concentrations were determined from their specific activities.

Preparation of exo$^-$ T7 DNA Polymerase. The plasmid pG5X, an expression vector for the exonuclease deficient phage T7 gene 5 protein (the catalytic subunit of T7 DNA polymerase) described by Patel et al. (1991), was obtained from Smita Patel (Ohio State University) and Kenneth Johnson (Pennsylvania State University). *Escherichia coli* A179/pGp1/pG5X cells were induced exactly as described (Patel et al., 1991). The purification scheme used was a variation of the published procedure (Patel et al., 1991); all steps were carried out as published until the ssDNA-cellulose column. For the present experiments, this column was substituted with a 100-mL phosphocellulose column (Whatman) equilibrated in P-cell buffer (20 mM K_2HPO_4, pH 7.4,

1 mM EDTA, 1 mM DTT, and 10% glycerol) with 50 mM KCl. The protein fraction (dialyzed against the same buffer) was loaded onto the column at a flow rate of 2 mL/min. The column was washed with an additional 100 mL of P-cell buffer + 50 mM KCl prior to starting a 1-L linear gradient of 50–500 mM KCl. The fractions containing gene 5 protein (eluting at approximately 200 mM KCl) were combined and diluted 2-fold in 10 mM Tris-HCl (pH 7.5) and 1 mM EDTA before loading onto an 80 mL DEAE-Bio-Gel A column previously equilibrated in 50 mM Tris-HCl (pH 7.5), 0.1 mM EDTA, 10% glycerol, 5 mM DTT, and 100 mM NaCl. The column was washed with 50 mL of the same buffer prior to starting an 800-mL linear gradient of 100–400 mM NaCl. Fractions containing gene 5 protein (eluting at 200–250 mM NaCl) were combined and dialyzed against storage buffer (50 mM Tris-HCl, pH 7.5, 0.1 mM EDTA, 50% glycerol, 5 mM DTT, and 50 mM KCl). The resultant protein is judged to be >90% pure on a Coomassie Blue stained SDS–polyacrylamide gel. The T7 exo$^-$ DNA polymerase was reconstituted immediately prior to use by mixing thioredoxin, the processivity subunit of T7 DNA polymerase (a kind gift of Sydney Edwards and Kenneth Johnson), in 5 mM DTT with the exo$^-$ gene 5 protein in a 20:1 molar ratio, as previously described (Patel et al., 1991).

Reaction Conditions. All reactions were carried out in a buffer containing 40 mM Tris-HCl (pH 7.5), 1 mM EDTA, 1 mM DTT, 0.1 mg/mL BSA, and 50 mM NaCl. $MgCl_2$ (12.5 mM, final) was added along with dNTPs to initiate the reactions. All reactions were performed at 20 ± 1 °C.

Quench-Flow. The quench-flow apparatus used was designed and built by Jean Gangloff and co-workers, as described (Gangloff et al., 1984). This instrument has a practical reaction time range of 11–600 ms which is adjusted by varying both the reaction tube length and the rotation speed of the cam used to push the pistons into the syringes. Prior to use for the presently described experiments, the timing of the quench-flow appuratus was tested by measuring the kinetics of hydrolysis of 2,4-dinitrophenyl acetate by concentrated base. The rate constants obtained were in good agreement with those previously reported (Gangloff et al., 1984). The reaction syringes A and B were loaded with 0.6 mL of enzyme–DNA and $MgCl_2$/dNTP solutions, respectively. The quench syringe was loaded with 1.2 mL of 0.6 M EDTA. From each reaction time course, 11 (~200 μL) quenched time points were obtained.

Experimental Design. For all experiments (except when the rate of enzyme–DNA binding was studied), 2× final concentrations of polymerase and 5′-labeled primer/template were allowed to come to equilibrium for 10 min in reaction buffer. To initiate the reaction, an equal volume of a 2× final concentration mixture of $MgCl_2$, dNTPs, and buffer was added. After the desired reaction time, EDTA (0.3 M, final) was added as a quench. This reaction scheme was followed whether the quench-flow apparatus was used or aliquots of the reaction were quenched manually. The quenched reaction aliquot from each time point was mixed 1:2 with de-ionized formamide and analyzed by denaturing gel electrophoresis using 20% sequencing gels. The substrate and product bands were quantitated using a Bio-imaging analyzer BAS 2000 (Fuji).

Data Analysis. All product vs time curves were fit to single exponentials using the KaleidaGraph program. All rate vs [dNTP] curves were fit to $v = V_{max}[dNTP]/K_m + [dNTP]$, the Michaelis–Menton equation, by the same program.

RESULTS

All of the kinetic studies of nucleotide incorporation presented below were carried out using an exo$^-$ derivative of T7 DNA polymerase and synthetic DNA primer/templates (see Table 1 for sequences). The exo$^-$ T7 DNA polymerase was used because the exonuclease activity of the wild-type enzyme is significantly faster than the rate of lesion bypass. In such reactions with the wild-type enzyme, only primer degradation, and not elongation, was detected (data not shown). The template strands used in all studies were identical, except for the presence or absence of an *N*-2-aminofluorene or *N*-2-acetylaminofluorene adduct covalently attached to the C8 position of the single guanine residue (see Figure 1 for structures). The three different primer strands used were all completely complementary to the template strand, differing only in length and therefore in distance between the 3′ end of the primer and the position of the single guanine in the template strand (see Table 1 for sequences). The 25/44-mer primer/templates were used in multiple incorporation studies to look at the rates of nucleotide addition before, opposite, and after the unmodified or modified guanine at position 31 of the template. The 30/44-mer and 31/44-mer primer/templates were used to look at the rates of single nucleotide incorporation opposite and after the guanine, respectively. For all reactions described in this paper, the 5′ end of the primer was labeled with ^{32}P, and the reaction time courses of primer extension were followed by denaturing polyacrylamide gel electrophoresis. The reaction conditions were specifically chosen to be similar to those Johnson and co-workers used to characterize the polymerization pathway of T7 DNA polymerase on unmodified DNA in order to test that the enzyme and the unmodified primer/templates used in the present studies acted as expected (Patel et al., 1991; Wong et al., 1991). In every case tested, the rates for correct incorporation and misincorporation using the unmodified primer/templates were within experimental error of the rates reported (see below).

Multiple Nucleotide Incorporation Studies. To gain an over-all understanding of how *N*-2-aminofluorene and *N*-2-acetylaminofluorene adducts affect the local rate of polymerization, reactions were performed in which dCTP, dTTP, and dGTP (200 μM each) were added to modified or unmodified 25/44-mer primer/templates (150 nM) with prebound exo$^-$ T7 DNA polymerase (100 nM). Under these conditions, any enzyme that dissociates from the elongated product DNA will be trapped by the excess primer/template. This is useful both (1) to ensure that during the early phase of the reactions polymerization is processive and (2) during the later phase to estimate the rate of enzyme–DNA dissociation. The presence of two dTs at positions 37 and 38 of the template and the absence of dATP in the reactions stopped the polymerization after 11 nucleotides, except for the misincorporation seen at long time points. The rates of nucleotide incorporation were followed in time courses ranging from 20 ms to 20 min. Reaction aliquots quenched at times ranging from 20 to 600 ms were obtained using a rapid quench-flow apparatus; reaction time points from 5 s to 20 min were stopped by hand. Figure 2 shows the results of selected reaction time points for each of the three reactions. Calculations of rate constants were done from complete time courses, containing 32 reaction time points each. Note that the time points shown in Figure 2 for the modified primer/templates are not the same as those shown for the unmodified.

For the unmodified 25/44-mer, the 100 nM enzyme prebound to 100 nM primer/template incorporated 11

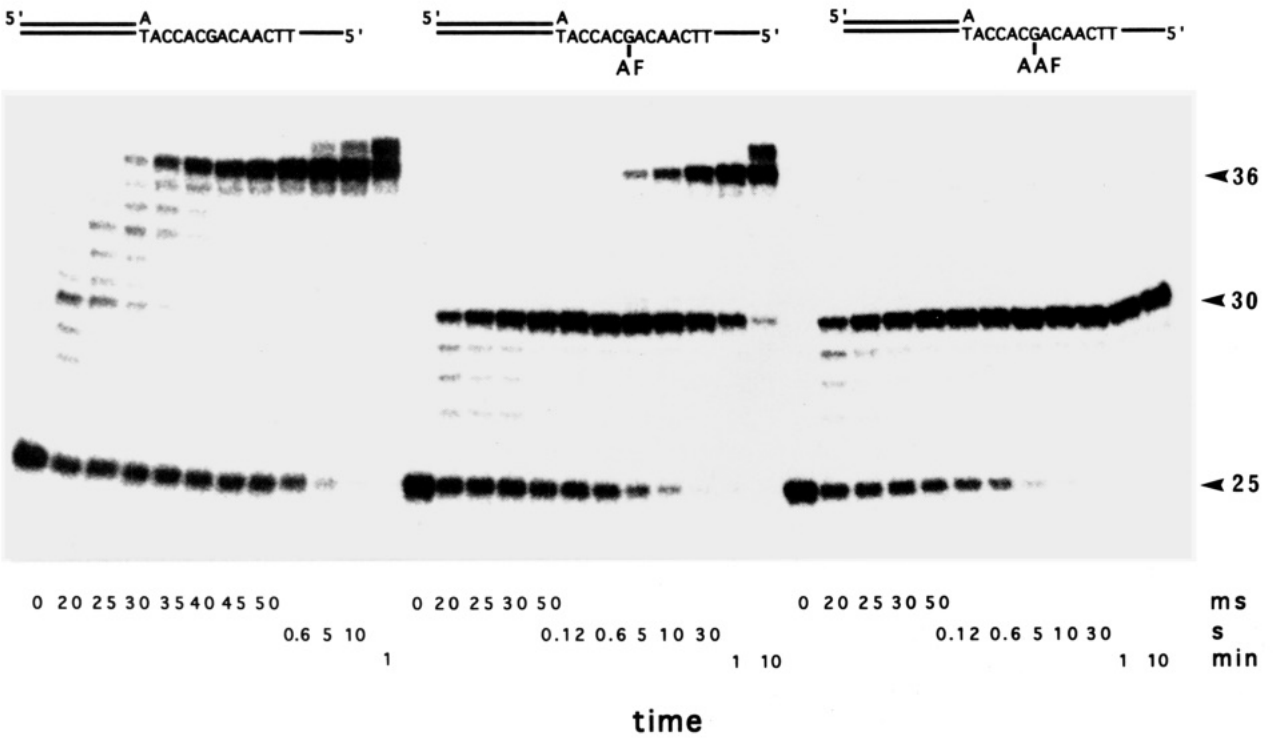

FIGURE 2: Primer extension reactions with 25/44-mer, 25/44-AF-mer, and 25/44-AAF-mer. The reactions were performed by mixing exo$^-$ T7 DNA polymerase (100 nM) and 5′-^{32}P-labeled primer/template (150 nM) with dCTP, dTTP, and dGTP (200 μM each), in standard reaction buffer as described under Experimental Procedures. The reactions were quenched at the indicated times by addition of EDTA (0.3 M final concentration) and analyzed by denaturing gel electrophoresis. The primer/template used in each experiment is represented by a schematic above each time course. The positions of intial 25-mer primer and the elongated 30- and 36-mer products are indicated to the right.

nucleotides with an approximate over-all rate constant of 28 s^{-1}, or an estimated average rate constant of 300 s^{-1} for each nucleotide. Incorporation of a nucleotide opposite the dG in the template is slightly slower than other incorporation events (note the dark band at 20 and 25 ms migrating at the 30-mer position). The rates of incorporation of individual nucleotides are known to vary, and the very slight pausing that is seen here is no different in magnitude than what has previously been seen in other sequence contexts (Patel et al., 1991). The extension of the 36-mer product primer to a 37-mer at long time points indicates that the polymerase misincorporated dCTP, dGTP, and/or dTTP opposite the dT at position 37. This rate of misincorporation is consistent with rates previously published (Wong et al., 1991). The constant level of remaining 25-mer primer that was not elongated within the early time points indicates that the reaction was indeed processive. The rate constant of disappearance of the 25-mer primer (by elongation to a more slowly migrating species) was determined to be 0.19 s^{-1}. This rate is equal to the rate of enzyme–DNA product dissociation plus the rates of enzyme–25/44-mer binding and elongation. Since the binding and elongation rates have previously been shown to be significantly faster than the dissociation rate (Patel et al., 1991), the rate of elongation from the remaining 25-mer is a rough estimate of the enzyme–product dissociation rate. The rate of dissociation estimated by this method (0.19 s^{-1}) is very similar to the previously determined rate of 0.2 s^{-1}.

When the template contained an *N*-2-aminofluorene adduct attached to the guanine at position 31, the kinetics of primer elongation look quite different. Incorporation to position 30, just before the lesion, occurred with an approximate over-all rate constant of 50 s^{-1} or an estimated average rate constant of 250 s^{-1}. Up to this position, the incorporation rate was very similar, within experimental error, to that seen with the unmodified DNA. From 50 ms until 0.6 s, very little further primer elongation was detected. The concentration of remaining 25-mer primer did not significantly change during this time period, indicating that no free polymerase bound to the remaining primer/template and, as described below, that therefore there was no rapid dissociation of the enzyme from the stalled complex. At 5 s and beyond, elongation from the stalled complex is evident. No major intermediate bands migrating between the 30-mer and 36-mer are present, indicating that the slowest step in the AF-dG bypass was incorporation of a nucleotide opposite the adduct. However, a longer exposure of the gel reveals a faint band at position 31, indicating that incorporation one nucleotide after the lesion must have also been slower than normal.

Extension of the primer/template containing the AAF-dG adduct looked similar to that with the AF-dG adduct, except that very little extension from position 30 occurred. At 20 min, a very faint band at position 31 was visible (data not shown), suggesting that some incorporation opposite the AAF-dG adduct occurred. When the reaction was repeated in the presence of 500 μM of each of the four dNTPs, the results were similar except that within 5 min a band at position 31, corresponding to incorporation opposite the adduct, was strongly visible (data not shown). At 60 min, bands at positions 32 and 44 (full length, in the presence of all four dNTPs) were also visible. The accumulation of 32-mer primer indicates that incorporation even two nucleotides past the position of the adduct is also a slow step.

If binding of polymerase to 25/44-AF-mer and 25/44-AAF-mer is approximately as rapid as to the unmodified primer/templates, then the rates at which the remaining 25-mer primer/templates (50 nM) are elongated should be estimates of the rates of enzyme dissociation from the primer/templates stalled at the position of the adduct. Rate of binding studies were carried out by incubating enzyme (25 nM) and buffer in one syringe of the rapid quench-flow apparatus and 25/44-mer (50 nM), dTTP (200 μM), $MgCl_2$, and buffer in the other syringe. The rates of single dTTP incorporation under

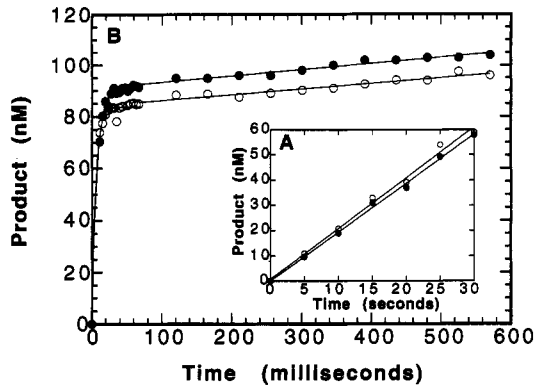

FIGURE 3: Steady-state and pre-steady-state correct single nucleotide incorporation into unmodified 30/44-mer and 31/44-mer primer/templates. (A) A preincubated solution of T7 DNA polymerase (exo⁻, 10 nM) and 5′-^{32}P-labeled unmodified primer template (400 nM), either 30/44 mer (●) or 31/44 mer (○), were mixed with the correct next dNTP (100 μM) (either dCTP or dTTP, respectively) in standard reaction buffer. The reactions were quenched by addition EDTA (0.3 M final). The reaction products were analyzed by denaturing gel electrophoresis and quantitated by phosphorimage analysis as described under Experimental Procedures. The data fit straight lines with slopes equal to 0.19 s^{-1} (●) and 0.21 (○) s^{-1} per enzyme active site. (B) This pre-steady-state experiment was performed just as the steady-state experiment shown in panel A, except that the enzyme to DNA concentrations were adjusted (100 nM exo⁻ T7 DNA polymerase; 200 nM primer/templates) and the rapid-quench appuratus was used. The data fit to biphasic curves with rate constants equal to 150 s^{-1} (●, 30/44-mer and dCTP) and 200 s^{-1} (○, 31/44-mer and dTTP) for the rapid phase and 0.2 s^{-1} for the slow phases.

these conditions were found to be 6.0, 5.0, and 6.6 s^{-1} for the unmodified, AF-dG, and AAF-dG primer/templates, respectively (data not shown). These results indicate that the presence of either adduct at position 31 does not significantly affect the rate of enzyme binding to, or initial elongation from, the 25/44-mer primer/template. Therefore, any polymerase that dissociated from the stalled complexes, Pol⁻30/44-AF-mer and Pol⁻30/44-AAF-mer, should have rapidly (on the time scale of the later time points) bound to and elongated from the remaining 25-mer primer. The rate constants of elongation from the remaining 25-mer primers were 0.11 and 0.16 s^{-1} for AF-dG and AAF-dG templates, respectively. For the AF-dG primer/template, the dissociation of enzyme could have been from either the stalled 30/44-mer complex or the fully elongated 36/44-mer complex, or both. Therefore, most simply, the rate of enzyme dissociation from the stalled complex is not greater than approximately 0.11 s^{-1}. In the reaction with the AAF-dG primer/template, the dissociation, with a rate constant of 0.16 s^{-1}, could only be from the stalled complex. These data imply that the T7 DNA polymerase stalls at the site of a bulky lesion approximately the same length of time that it stalls in the absence of the next correct nucleotide or at the end of a template, 5–10 s on average.

Single Nucleotide Incorporation Studies. All of the following experiments involved the incorporation of a single nucleotide into 30/44-mer and 31/44-mer primer/templates in order to gain an understanding of the polymerization reaction opposite or just after AF and AAF adducts. However, before working with the modified primer/templates, the identical unmodified primer/templates were tested to ensure that these substrates gave the expected reaction rates. The steady-steady rates of incorporating the correct nucleotides into unmodified 30/44-mer and 31/44-mer (dCTP and dTTP, respectively) were measured by using a large excess of primer/template (400 nM) over enzyme (10 nM). Figure 3A shows the time courses of dCTP and dTTP incorporation. The steady-state rate constants (the slopes divided by the enzyme concentration) are 0.19 and 0.21 s^{-1} for dCTP and dTTP incorporation into 30/44-mer and 31/44-mer, respectively.

The single-turnover rates of incorporation were estimated by using 100 nM exo⁻ T7 DNA polymerase, 200 nM 30/44-mer or 31/44-mer, and 100 μM dCTP or dTTP, respectively. The rapid-quench appuratus was used to stop the primer extension reactions at times ranging from 11 to 570 ms. The resulting biphasic time courses are shown in Figure 3B. The rapid phase of the time courses represents the first turnovers and have been fit to rate constants of 150 s^{-1} and 205 s^{-1} for dCTP and dTTP incorporation, respectively. However, since the earliest value is at 11 ms, these are only rough estimates of the actual rates. The second phase of the curves represents subsequent turnovers and are each fitted to rate constants of 0.2 s^{-1}, the same as the steady-state rate constants and the rate of polymerase–DNA dissociation determined from the multiple nucleotide incorporation experiments. As was previously shown (Patel et al., 1991), the steady-state rate of single nucleotide incorporation is limited by the rate of polymerase–DNA dissociation.

Finally, the rates of misincorporation of dATP into the unmodified primer/templates were determined. Using 100 nM enzyme, 100 nM 30/44-mer or 31/44-mer and 3 mM dATP, the rate constants for misincorporation were found to be 0.011 and 0.039 s^{-1}, respectively (data not shown). These are both within range of misincorporation rates previously determined using similar conditions (Wong et al., 1991).

Identity of Nucleotides Incorporated Opposite and Immediately after AF and AAF Adducts. In several different cell types, AF and AAF adducts cause varying levels of substitution mutations, often G → T transversions at the site of modification. Therefore, it was of interest to determine which nucleotides the exo⁻ T7 DNA polymerase would incorporate opposite and after the adducts. Preliminary time courses of the incorporation of each of the four dNTPs into each of the four modified primer/templates are shown in Figure 4. As seen in panel A, dCTP was most rapidly incorporated opposite AF-dG. Even at the first point shown, 0.1 min, significant levels of incorporation are seen. By 10 min, misincorporation of dCTP, opposite dA in the template, is also seen. dATP was also incorporated, but at a slower rate than dCTP. No dGTP or dTTP incorporation was detected. Immediately following the AF-dG adduct, the correct nucleotide, dTTP, was most rapidly incorporated (Figure 4, panel B). However, significant levels of dATP and barely detectable levels of dCTP and dGTP were also incorporated. It is interesting to note that the rate of misincorporation of dCTP starting from the 31-mer primer was approximately 5-fold slower than misincorporation of dCTP at the same position when the reaction was started with the 30-mer primer (i.e., compare the 32-mer band of the "C" reaction in Figure 4, panel A, with the faint 32-mer band appearing after 30 min of the "C" reaction in Figure 4, panel B).

As expected from the multiple nucleotide incorporation results, the rate of incorporation opposite AAF-dG is much slower than opposite AF-dG. However, under these reaction conditions (2 mM dNTP), incorporation of both dATP and dCTP are seen (Figure 4, panel C). No incorporation of dGTP or dTTP is detected. Interestingly, immediately following the AAF-dG modification, misincorporation of dATP is the favored event (Figure 4, panel D), with only a very low level of correct dTTP incorporation detected after long exposure times.

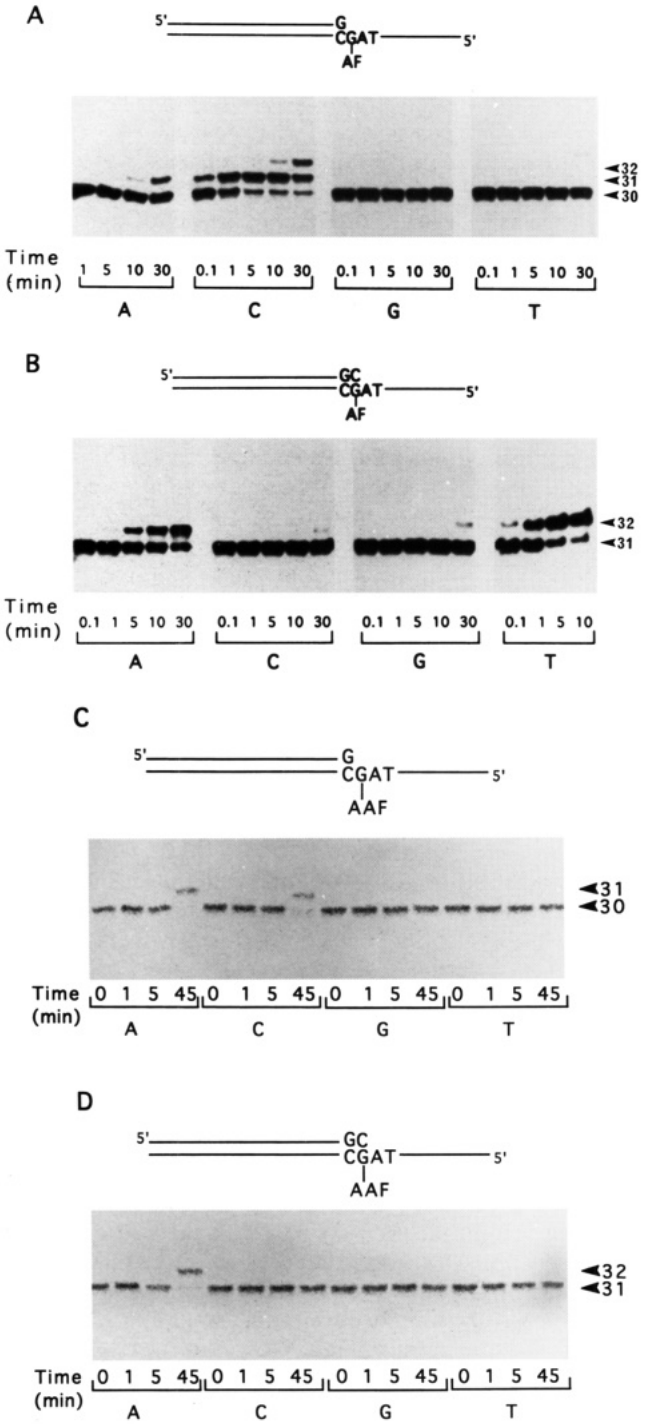

FIGURE 4: Determination of which dNTPs are incorporated opposite and immediately after AF-dG and AAF-dG in the templates. Aliquots of standard reactions containing 200 nM exo⁻ T7 DNA polymerase, 200 nM 5′-^{32}P-labeled modified primer/template (as indicated by the schematic above each panel), and 2 mM of the indicated dNTP, were quenched at the indicated times by addition of EDTA (0.3 M final concentration) and analyzed by denaturing gel electrophoresis as described under Experimental Procedures. The positions of the primer substrate and elongation products are indicated to the right of the samples.

Single- and Multiple-Turnover Kinetics of Single Nucleotide Addition. As seen in Figure 3B, the time course of single-nucleotide incorporation into unmodified primer/templates is biphasic. A rapid burst of product formation, equal to the concentration of active exo⁻ T7 DNA polymerase bound to the DNA, is seen in the first few milliseconds. This burst is followed by a second, much slower rate of product formation. The rate of the burst is a measure of the slow step

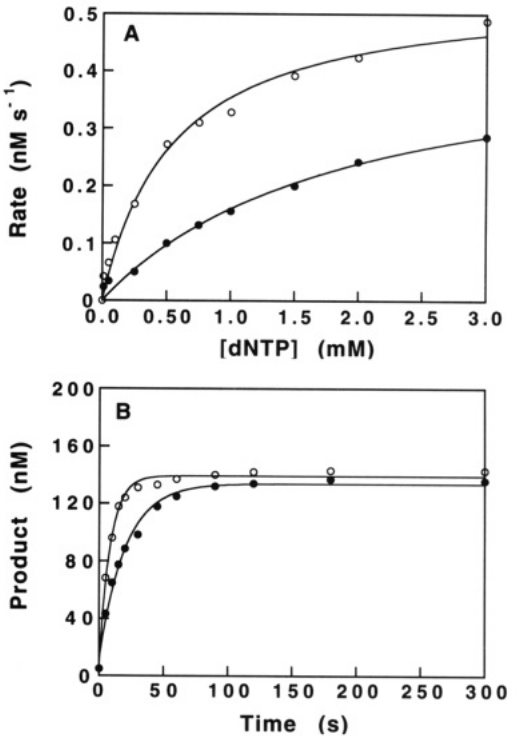

FIGURE 5: Steady-state and pre-steady-state rates of correct nucleotide incorporation opposite and immediately after AF-dG in the template. (A) The rates of single dCTP incorporation into 30/44-AF (●) and single dTTP incorporation into 31/44-AF (○) were measured from standard reactions that included 5 nM exo⁻ T7 DNA polymerase, 200 nM primer/template, and a dNTP concentration ranging from 25 μM to 3 mM. The data were fitted to the Michealis–Menton equation, $v = V_{max}[dNTP]/K_m + [dNTP]$. k_{cat} was calculated by dividing V_{max} by the polymerase concentration. (B) Pre-steady-state time points of single dCTP incorporation into 30/44-AF (●) and single dTTP incorporation into 31/44-AF (○) were taken from standard reaction mixes containing 150 nM polymerase, 150 nM primer/template, and 1 mM dNTP. The rate constants determined by fitting the data to single exponentials are 0.047 and 0.11 s^{-1} for dCTP and dTTP incorporation, respectively.

in single turnover, hypothesized to be a conformational change in the ternary complex (Johnson, 1992). The rate of the second phase corresponds to the rate of enzyme–DNA dissociation, the slow step in multiple-turnover reactions.

To determine whether the kinetics of nucleotide incorporation into the modified primer/templates resembles unmodified, the single- and multiple-turnover rates of addition of those nucleotides shown to be significantly incorporated were measured. Figure 5 shows the results for incorporation of dCTP opposite AF-dG in the 30/44-AF primer/template and dTTP immediately after AF-dG in the 31/44-AF primer/template. Multiple-turnover reactions were carried out using 5 nM exo⁻ T7 DNA polymerase, 200 nM primer/template, and a range of dCTP or dTTP concentrations. A plot of the rates determined vs [dNTP] used is shown in Figure 5, panel A. The apparent second-order rate constants, k_{cat}/K_m, were calculated to be 50 and 200 M^{-1} s^{-1} for incorporation of dCTP and dTTP into the 30/44-AF and 31/44-AF primer/templates, respectively. The single-turnover counterparts of the same reactions had 150 nM enzyme, 150 nM 30/44-AF or 31/44-AF, and 1 mM dCTP or dTTP, respectively, and are shown in Figure 5, panel B. The progress curves for these reactions are monophasic and fit well to a single exponential. This does not appear to be due to a significantly higher K_d or slower k_{on} rate (the k_{off} rate was already shown not to be significantly different for the modified DNA) for the enzyme and modified DNA, as higher protein and DNA concentrations

Table 2: Kinetic Constants of Single Nucleotide Incorporation

primer/template	dNTP	k_{cat} (s^{-1})	K_m (mM)	k_{cat}/K_m (M^{-1} s^{-1})
30/44-AF	dCTP[a]	9.4×10^{-2}	1.9	50
(═══G CGAT—) AF	dATP[b]	7×10^{-4}	6	0.1
31/44-AF	dTTP[a]	0.11	0.6	200
(═══GC CGAT—) AF	dATP[b]	1.9×10^{-3}	1.3	1.5
30/44-AAF	dCTP[b]	1.7×10^{-3}	3	0.6
(═══G CGAT—) AAF	dATP[b]	1.9×10^{-3}	1.5	1.3
31/44-AAF				
(═══GC CGAT—) AAF	dATP[b]	1×10^{-2}	8	1.3

[a] For these substrates, the constants k_{cat}, K_m, and k_{cat}/K_m were determined from reactions including 5 nM polymerase, 200 nM primer/template, and concentrations of dNTP ranging from 25 μM to 3 mM. [b] As in footnote *a*, except for this set of substrates the polymerase concentration was 200 nM and the DNA concentration was 400 nM.

and longer preincubation times did not affect the results (data not shown). The single-turnover rate constants (0.047 and 0.11 s^{-1}, for dCTP and dTTP incorporation into 30/44-AF and 31/44-AF, respectively) are approximately equal to the steady-state rate constants calculated from the k_{cat}/K_m values at 1 mM dNTP (0.05 and 0.2 s^{-1}, respectively). Within experimental error, the single- and multiple-turnover rate constants were found to be the same for all of the pairs of dNTPs and modified primer/templates listed in Table 2. The fact that the rate during the first turnover is the same as for subsequent turnovers indicates that enzyme–DNA dissociation is not rate-limiting in multiple-turnover reactions of incorporating a nucleotide opposite or immediately after AF-dG or AAF-dG. These, along with the multiple nucleotide incorporation results, also indicate that, unlike correct incorporation into unmodified primer/templates, the rate of dNTP incorporation opposite or just after either adduct is of the same order as, or is significantly slower than (depending on the adduct and [dNTP]), the enzyme–DNA dissociation rate.

The k_{cat}, K_m, and k_{cat}/K_m values for single nucleotide incorporation into each of the modified primer/templates are shown in Table 2. A higher enzyme to DNA ratio (200 nM/400 nM) was used to measure the rates of incorporation of dATP opposite or after AF-dG and in all AAF-dG experiments in order to improve the accuracy of following these slow reactions. For comparison, the k_{cat}/K_m values previously determined for correct incorporation and misincorporation into unmodified primer/templates are 1.5×10^7 and 20 $M^{-1}s^{-1}$, respectively (Wong et al., 1991). These values were determined for a separate primer/template substrate, so they should be considered as order of magnitude estimates when compared to the values from the present study.

The rates of nucleotide incorporation into unmodified and AF- and AAF-modified primer/templates can be compared at an approximately physiological dNTP concentration of 100 μM. The rate constant for correct nucleotide incorporation into unmodified primer/templates at 100 μM dNTP was previously shown to be 250 ± 100 s^{-1} (Patel et al., 1991; Wong et al., 1991). From the k_{cat}/K_m values (the apparent second-order rate constants) reported in Table 2, the rate constants for correct incorporation opposite either AF-dG or AAF-dG at 100 μM dCTP are calculated to be 5×10^{-3} and 6×10^{-5} s^{-1}, respectively. Therefore, dCTP is incorporated approximately 5×10^4-fold and 4×10^6-fold more rapidly opposite dG than opposite AF-dG and AAF-dG, respectively. However, the differences in the rates of dATP misincorporation between unmodified and modified primer/templates are not as large; the rate constant previously determined for misincorporation of a single nucleotide into an unmodified primer/template is 2×10^{-3} s^{-1} at 100 μM dNTP (Wong et al., 1991), whereas incorporation of dATP opposite AF-dG and AAF-dG occurs with rate constants of 1×10^{-5} and 1×10^{-4} s^{-1}, respectively.

It should be noted that the calculated rates of correct single nucleotide incorporation opposite and after the AF adduct at 200 μM dNTP (0.01 and 0.04 s^{-1}, respectively) are slower than what was predicted from the multiple nucleotide incorporation experiments ($\sim$0.05 and $>$0.05 s^{-1}, respectively). This discrepancy ($\sim$5-fold) between the single and multiple nucleotide incorporation rates is similar to that noted in the previous section for the rates of dCTP misincorporation after AF-dG when it was the first vs the second nucleotide incorporated (Figure 4, panels A and B). At the present time it is not known whether this phenomenon of incorporating each nucleotide faster when more than one is being incorporated is due to an intrinsic property of T7 DNA polymerase bypass of AF lesions or is a slight artifact caused by the reaction conditions. Therefore, the rates of nucleotide incorporation presented here should be considered as estimates of the actual bypass rates.

DISCUSSION

The presence of an AF or AAF adduct on a DNA template does not significantly affect the rate of primer extension by T7 DNA polymerase (exo$^-$) until the polymerase must incorporate a nucleotide directly opposite the lesion. Incorporation of dCTP opposite AF-dG and AAF-dG is reduced $\sim 5 \times 10^4$- and $\sim 4 \times 10^6$-fold, respectively, relative to opposite dG in the primer/templates (at the approximately physiological dCTP concentration of 100 μM). Incorporation of the next correct nucleotide after the lesion is also slower than normal ($\sim 1 \times 10^4$- and $> 1 \times 10^7$-fold slower, for AF-dG and AAF-dG containing primer/templates, respectively). The presence of either adduct disrupts the processivity of the polymerase; although the enzyme–DNA dissociation rate is not greatly perturbed by the adducts, the rate of nucleotide incorporation opposite either adduct is generally slower than dissociation. These results are summarized in a simplified reaction scheme shown in Figure 6.

Discrimination between correct and incorrect nucleotides incorporated by the polymerase [defined as: $\{(k_{cat}/K_m)_{correct} + (k_{cat}/K_m)_{incor.}\}/(k_{cat}/K_m)_{incor.}$] is a major component of the fidelity of a polymerase and is affected by the presence of AF and AAF adducts. T7 DNA polymerase normally discriminates $\sim 7.5 \times 10^5$-fold between incorporation of correct and incorrect nucleotides (Wong et al., 1991). This discrimination is reduced to $\sim$500- fold and $\sim$100-fold opposite and immediately after AF-dG, respectively, where the favored incorrect nucleotide is dATP. Misincorporation of dATP is the favored event opposite and immediately after AAF-dG.

The structure of double-stranded DNA is affected very differently by the presence of AF-dG vs AAF-dG (Daune et al., 1981). Biophysical (Evans et al., 1980; Leng et al., 1980; Santella et al., 1980) and enzymatic probing studies (Kriek & Spelt, 1979; Sage et al., 1979) have indicated that AF-dG has very little effect on the overall structure of the double helix. The NMR structure of a duplex, in which dA is opposite the AF-dG, revealed that the AF-dG is in the syn conformation

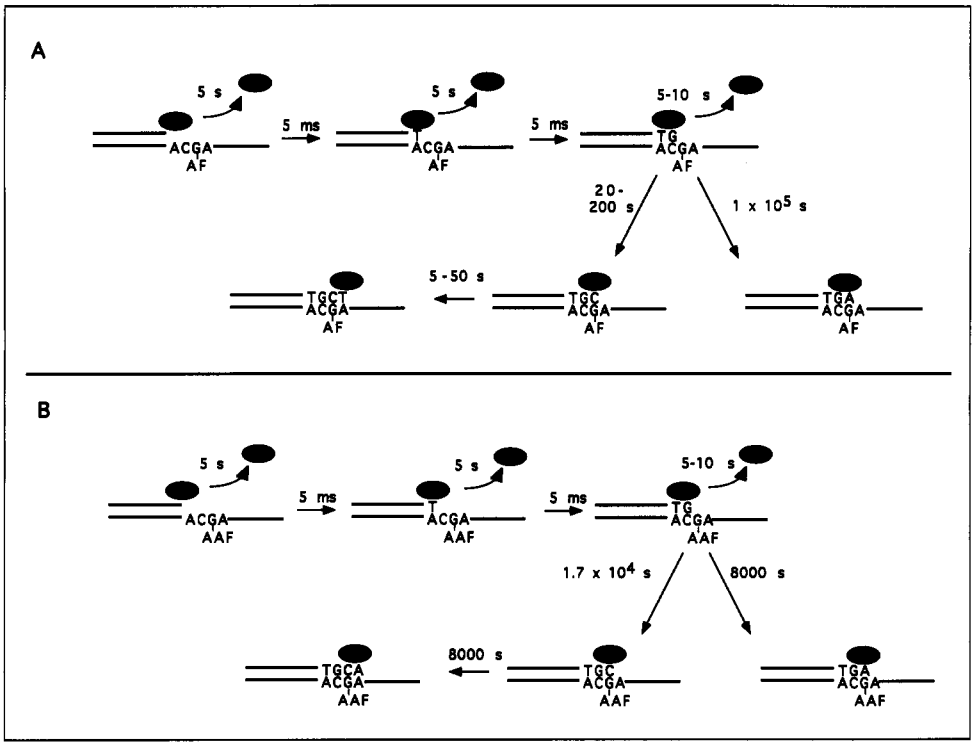

FIGURE 6: A simplified reaction scheme showing the approximate overall times of nucleotide incorporation (and polymerase dissociation) as the polymerase approaches and bypasses (A) AF and (B) AAF adducts. The T7 DNA polymerase (exo$^-$) is represented by a black oval. The rates were calculated at dNTP concentrations of 100 μM from k_{cat}/K_m values. A range of values is given for correct nucleotide incorporation opposite and after the AF because of the slight discrepancy in rates seen for the multiple nucleotide and single nucleotide incorporation experiments.

with the AF ring in the minor groove away from the helix axis (Norman et al., 1989). On the other hand, AAF adducts have been shown to induce major changes in the DNA conformation. When AAF-dG is located within a random sequence, it causes local denaturation of the DNA, with the guanine rotated outside of the double helix and the AAF ring stacked between neighboring base pairs (Fuchs & Daune 1971; O'Handley et al., 1993). This structure has been referred to as either the "insertion–denaturation" or the "base displacement"model (Fuchs & Daune 1972; Fuchs et al., 1976; Grunberger & Weinstein, 1979).

Not surprisingly, these different adduct-induced DNA structures are reflected in dramatically different biological properties exhibited by AF and AAF in terms of (1) toxicity/survival, (2) SOS inducing properties in *E. coli*, and (3) mutagenic specificity. (1) The relative toxicity of these adducts can be estimated quantitatively by measuring the number of adducts bound per plasmid that reduces the transformation efficiency of the plasmid to 37% (representing a single lethal hit in terms of Poisson statistics). When transformed into a repair-deficient *urvA E. coli* strain, ~60 AF or ~4–5 AAF adducts are required to reduce the transformation efficiency to 37% (Fuchs & Seeberg 1984). The toxicity effects of AAF adducts are similar to those of UV-induced photodimers (Schmid et al., 1982). (2) AAF adducts, but not AF adducts, efficiently trigger the SOS response in bacteria (Salles et al., 1983). Again, AAF and UV lesions exhibit a quantitatively similar SOS-inducing capacity (Salles et al., 1983). Since the SOS response is thought to result from a transient block in DNA replication induced by DNA lesions, these data suggest that AF lesions are bypassed more readily than AAF lesions or UV photodimers *in vivo*. (3) In all cell types studied, AF adducts have been found to induce primarily targeted G·C → T·A transversions (Bichara & Fuchs 1985; Mah et al., 1989). In *E. coli*, AAF adducts primarily induce frame-shift mutations (Fuchs et al., 1981; Koffel-Schwartz et al., 1984). These mutations are mainly found when the AAF-dG is located within a run of guanines (Lambert et al., 1992) or is at the G_3 position of a *Nar*I restriction enzyme recognition site (G_1G_2-CG_3CC) (Burnouf et al., 1989).

The three above biological effects of AF and AAF adducts (toxicity, SOS induction, and mutagenesis) are most likely all results of the same phenomenon: perturbation of DNA replication. Therefore it is of interest to understand how replicative bypass of the adducts differs from normal replication, and how bypass of the two lesions differ from each other. It was previously found that AAF but not AF adducts block DNA replication *in vitro* (Strauss & Wang, 1990). However, the rate at which a polymerase incorporates nucleotides as it approaches, is just opposite, or is just passed the adducts has not before been studied. In this work we show that AF adducts impede replication very significantly, even though *in vivo* they are not strongly toxic lesions. The average rate of dCTP incorporation opposite the AF-dG (~200 s per event) is about 5 × 10^4-fold slower than incorporation opposite dG (~4 ms per event), at 100 μM dCTP. In addition, incorporation of the next nucleotide is also a slow process. As yet, we do not know at what position after the adduct the polymerase resumes its normal rate of nucleotide incorporation. For AAF adducts, the bypass reaction is ~100-fold slower than for AF adducts, which may explain their significantly greater toxicity. At least for the polymerase used in these studies, the enzyme–DNA dissociation rate is significantly faster than the AAF bypass rate. *In vivo* this may result in the generation of daughter strand gaps that could trigger the SOS response.

The G → T mutation specificity that is observed *in vivo* for AF adducts in *E. coli* and in human cells is reflected in the present work by the relatively high frequency of dATP incorporation opposite the adduct-containing guanine. The

dA/dC incorporation ratio (~1/500) by exo⁻ T7 DNA polymerase opposite AF-dG is in good agreement with our previous estimation of the efficiency of conversion of an AF adduct into a mutation in *E. coli* (~1/2000) (Bichara & Fuchs, 1985). Since this conversion efficiency was determined from a forward mutation spectrum where a large proportion of the mutations are phenotypically silent, it is an underestimation by at least a factor of 3. Interestingly, increased *in vivo* substitution mutagenesis frequencies targeted immediately after AF-dG or AAF-dG have not been reported and yet might be expected from the present results. At this time it is not possible to say if the decrease in correct nucleotide vs dATP discrimination after the lesions is peculiar to the exo⁻T7 DNA polymerase, to the particular primer/template sequences chosen, or to other aspects of the *in vitro* reactions.

The observation that replication speed is slow even after incorporation opposite the adduct site may also have some important implications in terms of mutagenesis. We have recently observed that single AAF adducts are able to trigger −1 frame-shift mutations within a sequence of three C's located 5′ of the AAF adduct on the template strand (Lambert et al., 1992). These semitargeted mutations may be caused by slippage within the three C's that is favored as a consequence of the slow adduct bypass rate.

The studies described in this paper are a start to understanding the detailed mechanism by which a DNA polymerase bypasses a bulky adduct in the DNA. At the present time, pre-steady-state kinetic measurements of the kind described here can only be done with a few simple polymerases for which large quantities can be purified. How AF-dG and AAF-dG alter the nucleotide incorporation rates, extents, and discrimination of bacterial and eukaryotic replicative polymerase complexes is a fascinating question for future biochemical and genetic studies.

ACKNOWLEDGMENT

We thank K. Johnson and S. Patel for helpful discussions and for sharing their exo⁻ T7 DNA polymerase expression vector, J. Gangloff for assistance with the rapid-quench instrument, P. Belguise-Valladier for assistance in preparing the modified DNA templates, and M. Bichara for technical assistance.

REFERENCES

Belguise-Valladier, P., & Fuchs, R. P. P. (1994) *J. Mol. Biol.* (in press).

Bichara, M., & Fuchs, R. P. P. (1985) *J. Mol. Biol. 183*, 341–351.

Burnouf, D., Koehl, P., & Fuchs, R. P. P. (1989) *Proc. Natl. Acad. Sci. U.S.A. 86*, 4147–4151.

Donlin, M. J., Patel, S. S., & Johnson, K. A. (1991) *Biochemistry 30*, 538–546.

Daune, M., Fuchs, R. P. P., & Leng, M. (1981) *J. Natl. Cancer Inst. 58*, 201–210.

Evans, F., Miller, D., & Beland, F. (1980) *Carcinogenesis 1*, 955–959.

Fuchs, R. P. P. (1984) *J. Mol. Biol. 177*, 173–180.

Fuchs, R. P. P., & Daune, M. (1971) *FEBS Lett. 14*, 206–208.

Fuchs, R. P. P., & Daune, M. (1972) *Biochemistry 11*, 2659–2666.

Fuchs, R. P. P., & Seeberg, E. (1984) *EMBO J. 3*, 757–760.

Fuchs, R. P. P., LeFevre, J. F., Pouyet, J., & Daune, M. (1976) *Biochemistry 15*, 3347–3351.

Fuchs, R. P. P., Schwartz, N., & Daune, M. P. (1981) *Nature 294*, 657–659.

Gangloff, J., Pouyet, J., Kern, D., & Dirheimer, G. (1984) *J. Biochem. Biophys. Methods 9*, 201–213.

Grunberger, D., & Weinstein, J. B. (1979) *Chemical Carcinogen and DNA*, pp 59–93, CRC Press, Boca Raton, FL.

Johnson, K. A. (1992) *Phil. Trans. R. Soc. Lond. B 336*, 107–112.

Koehl, P., Burnouf, D., & Fuchs, R. P. P. (1989) *J. Mol. Biol. 207*, 355–364.

Koffel-Schwartz, N., Verdier, J. M., Bichara, M., Freund, M., Daune, M. P., & Fuchs, R. P. P. (1984) *J. Mol. Biol. 177*, 33–51.

Kriek, E. (1992) *J. Cancer Res. Clin. Oncol. 118*, 481–489.

Kriek, E., & Spelt, C. E. (1979) *Cancer Lett. 7*, 147–154.

Lambert, I. B., Napolitano, R. L., & Fuchs, R. P. P. (1992) *Proc. Natl. Acad. Sci. U.S.A. 89*, 1310–1314.

Leng, M., Ptak, M., & Rio, P. (1980) *Biochem. Biophys. Res. Commun. 96*, 1095–1102.

Mah, M. C.-M., Maher, V. M., Thomas, H., Reid, T. M., King, C. M., & McCormick, J. J. (1989) *Carcinogenesis 10*, 2321–2328.

Mah, M. C.-M., Boldt, J., Culp, S. J., Maher, V. M., & McCormick, J. J. (1991) *Proc. Natl. Acad. Sci. U.S.A. 88*, 10193–10197.

Michaels, M. L., Johnson, D. L., Reid, T. M., King, C. M., & Romano, L. J. (1987) *J. Biol. Chem. 262*, 14648–14654.

Michaels, M. L., Reid, T. M., King, C. M., & Romano, L. J. (1991) *Carcinogenesis 12*, 1641–1646.

Norman, D., Abuaf, P., Hingerty, B. E., Live, D., Grunberger, D., Broyde, S., & Patel, D. J. (1989) *Biochemistry 28*, 7462–7476.

O'Conner, D., & Stohrer, G. (1985) *Proc. Natl. Acad. Sci. U.S.A. 82*, 2325–2329.

O'Handley, S. F., Sanford, D. G., Xu, R., Lester, C. C., Hingerty, B. E., Broyde, S., & Krugh, T. R. (1993) *Biochemistry 32*, 2481–2497.

Patel, S. S., Wong, I., & Johnson, K. A. (1991) *Biochemistry 30*, 511–525.

Sage, E., Spodheim-Maurizot, M., Rio, P., Leng, M., & Fuchs, R. P. P. (1979) *FEBS Lett. 108*, 66–68.

Salles, B., Lang, M. C., Freund, A. M., Paoletti, C., Daune, M., & Fuchs, R. P. P. (1983) *Nucleic Acids Res. 11*, 5235–5242.

Santella, R., Kriek, E., & Grunberger, D. (1980) *Carcinogenesis 1*, 897–902.

Schmid, S. E., Daune, M. P., & Fuchs, R. P. P. (1982) *Proc. Natl. Acad. Sci. U.S.A. 79*, 4133–4137.

Shibutani, S., Gentles, R., Johnson, F., & Grollman, A. P. (1991) *Carcinogenesis 12*, 813–818.

Strauss, B. S., & Wang, J. (1990) *Carcinogenesis 11*, 2103–2109.

Wong, I., Patel, S. S., & Johnson, K. A. (1991) *Biochemistry 30*, 526–537.